melanotic coating of abiotic Sephadex beads injected into the mosquito thorax (*12*). Interestingly, neither parasite nor bead encapsulation mapping experiments identified any locus within the *2La* region. The reported association of $2L+^a$ with refractoriness (*3*) may be an artifact of the previously available strains (for example, a result of suppression of recombination). It is also possible that a locus within the *2La* region is required for the expression of *Pen1*, *Pen2*, and *Pen3* but is not directly involved in encapsulation. The new strains are both $2L+^a/+^a$ and may already carry the same permissive allele at this locus.

Melanotic encapsulation is only one of several types of refractoriness of anopheline mosquitoes to *Plasmodium* parasites (*13*). Another common type is manifested earlier, before or during parasite invasion of the midgut epithelium (*14*). Two QTLs each have been identified for the susceptibility of *Aedes aegypti* mosquitoes to *P. gallinaceum* (*15*) and Brugian worms (*16*). However, these *Ae. aegypti* QTLs control the intensity of parasite infection and thus differ from the *Pen* loci of *A. gambiae*. Hence, our results establish that the development of malaria parasites can be blocked by two independent refractory mechanisms that are both temporally and functionally different.

The nature of *Pen1*, *Pen2*, and *Pen3* is not known, although *Pen3* maps in the general area where the prophenoloxidase gene is also located (*17*). In any case, the detailed localization of genes involved in the *A. gambiae* encapsulation response offers the opportunity to clone these genes positionally and to characterize the antiparasitic immune response of this vector at both the genetic and molecular levels.

REFERENCES AND NOTES

1. F. H. Collins *et al.*, *Science* **234**, 607 (1986).
2. M. Coluzzi *et al.*, *Trans. R. Soc. Trop. Med. Hyg.* **73**, 483 (1979).
3. K. D. Vernick and F. H. Collins, *Am. J. Trop. Med. Hyg.* **40**, 593 (1989); A. E. Crews-Oyen *et al.*, *ibid.* **49**, 341 (1993).
4. The new refractory strain (L35) was derived from the previous one (*1*) and is homozygous for *collarless* (*7*). The new susceptible strain (4Ar/r) is homozygous for *pink-eye* and *red-eye* [C. B. Beard *et al.*, *J. Hered.* **86**, 375 (1995)] and polymorphic for *collarless*. Both L35 and 4Ar/r are polymorphic for the *2Rbc* inversion but are fixed for $2L+^a$, *Xag* inversion of the X chromosome and the standard chromosome 3 karyotype.
5. F. H. Collins and A. J. Cornel, unpublished data.
6. Collarless (*c/c*) F_1 females were generated from a mass mating between L35 males and 4Ar/r females. Each was singly mated with one collared susceptible (either *C/c* or *C/C*), collarless susceptible (*c/c*), or collarless refractory male. These females were allowed to blood-feed on a *P. cynomolgi* B–infected rhesus monkey. After a single oviposition, the normal and encapsulated oocysts in the midgut of each female were counted 5 to 6 days later. The heterozygosity of some microsatellite markers in the susceptible strain allowed mapping of *collarless* in families E4 and E5 (*7*). Each BC family was individually reared, and the emerging females were allowed to blood-feed on another infected rhesus monkey. Infection and encapsulation phenotypes of the midgut were determined as above. The remaining carcasses were frozen for genomic DNA preparation and microsatellite genotyping.
7. L. Zheng, F. H. Collins, V. Kumar, F. C. Kafatos, *Science* **261**, 605 (1993); G. Dimopoulos *et al.*, *Genetics* **143**, 953 (1996); L. Zheng, M. Q. Benedict, A. Cornel, F. H. Collins, F. C. Kafatos, *ibid.*, p. 941.
8. Fluorescent microsatellite genotyping was carried out as described [D. C. Mansfield *et al.*, *Genomics* **24**, 225 (1994)] with an ALF DNA sequencer (Pharmacia). The data were analyzed with Fragment Manager (Pharmacia). Genotyping of randomly selected mosquitoes was repeated to verify the quality of the data.
9. E. Lander *et al.*, *Genomics* **1**, 174 (1987); A. Paterson *et al.*, *Nature* **335**, 721 (1988).
10. A genetic map was generated from the combined genotype data from families E1 to E5. QTL mapping was performed on individual and combined families E1 to E5 with the markers shown in Fig. 2 and for selected markers on E6 and E7. A LOD score of 3.0 was used as the minimum for declaring the existence of a QTL. After the highest value QTLs in chromosomes 2 and 3 (*Pen1* and *Pen2*) were fixed, the residual variations were mapped, revealing only one additional significant QTL, *Pen3*. Maximum likelihood estimates were also calculated in families E1 to E7 for markers listed in Table 1 (*9*). A similar genetic map order was also obtained with the program Joinmap [P. Stam, *Plant J.* **5**, 739 (1993)].
11. M. J. Gorman *et al.*, *Genetics*, in press.
12. M. J. Gorman *et al.*, *Exp. Parasitol.* **84**, 380 (1996).
13. A. Warburg and L. H. Miller, *Parasitol. Today* **7**, 179 (1991).
14. H. M. Al-Mashhadani, G. Davidson, C. F. Curtis, *Trans. R. Soc. Trop. Med. Hyg.* **74**, 585 (1980); P. M. Graves and C. F. Curtis, *Ann. Trop. Med. Parasitol.* **76**, 633 (1982); M. Shahabuddin *et al.*, *Exp. Parasitol.* **81**, 386 (1995); K. D. Vernick *et al.*, *ibid.* **80**, 583 (1995).
15. W. L. Kilama and G. B. Craig Jr., *Ann. Trop. Med. Parasitol.* **63**, 419 (1969); D. W. Severson *et al.*, *Genetics* **139**, 1711 (1995).
16. W. W. MacDonald and C. P. Ramachandran, *Ann. Trop. Med. Parasitol.* **59**, 64 (1965); D. W. Severson *et al.*, *Insect Mol. Biol.* **3**, 67 (1994).
17. W.-J. Lee *et al.*, unpublished data.

18. We thank S. Winkler, C. Schwager, R. Saffrich, U. Nentwich, and J. Stegemann for help in genotyping, and W. Collins, J. Sullivan, and C. Morris for help with rhesus monkeys. Supported by the John D. and Catherine T. MacArthur Foundation and the UNDP/World Bank/WHO Special Programme for Research and Training in Tropical Diseases (TDR). Experiments with rhesus monkeys were performed under the guidelines of CDC animal use protocol 676-COL-MON-CH.

26 December 1996; accepted 26 February 1997

Prevention of Lysosomal Storage in Tay-Sachs Mice Treated with *N*-Butyldeoxynojirimycin

Frances M. Platt,* Gabrielle R. Neises, Gabriele Reinkensmeier, Mandy J. Townsend, V. Hugh Perry, Richard L. Proia, Bryan Winchester, Raymond A. Dwek, Terry D. Butters

The glycosphingolipid (GSL) lysosomal storage diseases result from the inheritance of defects in the genes encoding the enzymes required for catabolism of GSLs within lysosomes. A strategy for the treatment of these diseases, based on an inhibitor of GSL biosynthesis *N*-butyldeoxynojirimycin, was evaluated in a mouse model of Tay-Sachs disease. When Tay-Sachs mice were treated with *N*-butyldeoxynojirimycin, the accumulation of G_{M2} in the brain was prevented, with the number of storage neurons and the quantity of ganglioside stored per cell markedly reduced. Thus, limiting the biosynthesis of the substrate (G_{M2}) for the defective enzyme (β-hexosaminidase A) prevents GSL accumulation and the neuropathology associated with its lysosomal storage.

The GSL storage diseases (*1*) result from the inheritance of defects in the genes encoding the catabolic enzymes required for the complete breakdown of GSLs within lysosomes. Possible strategies for the treatment of these debilitating and often fatal diseases include enzyme replacement therapy, gene therapy, substrate deprivation, allogeneic bone marrow transplantation, and palliative measures (*2*). Of these, symptomatic management is the only approach for treating most of these disorders, although transplantation techniques have been applied to some of these diseases. Currently, only the type 1 form of Gaucher disease, which is characterized by glucocerebrosidase deficiency in the absence of neuropathology, has been successfully treated by enzyme replacement therapy (*3*, *4*). However, skeletal abnormalities associated with the disease respond slowly to this treatment (*4*), and the neuropathologic forms of the

F. M. Platt, G. Reinkensmeier, R. A. Dwek, T. D. Butters, Glycobiology Institute, Department of Biochemistry, University of Oxford, South Parks Road, Oxford OX1 3QU, UK.
G. R. Neises, Monsanto Company, 700 Chesterfield Village Parkway, St. Louis, MO 63198, USA.
M. J. Townsend and V. H. Perry, Department of Pharmacology, University of Oxford, Mansfield Road, Oxford OX1 3QT, UK.
R. L. Proia, National Institute of Diabetes and Digestive and Kidney Diseases, National Institutes of Health, Bethesda, MD 20892, USA.
B. Winchester, Institute of Child Health, 30 Guilford Street, London WC1N 1EH, UK.

*To whom correspondence should be addressed. E-mail: fran@oxglua.glycob.ox.ac.uk

disease (types 2 and 3) are refractory to therapy. The therapeutic prospects for this rare group of disorders are therefore extremely limited, and new strategies are urgently needed.

One approach that may be generally applicable to the GSL storage disorders, irrespective of the specific gene defect involved, is substrate deprivation. This method would use a specific inhibitor of GSL biosynthesis to partially reduce the amounts of GSLs synthesized by cells. This would then permit the residual activity of the defective enzyme to fully catabolize the GSLs synthesized, thus preventing accumulation. We discovered a specific inhibitor of the glucosyltransferase-catalyzed biosynthesis of glucosylceramide (GlcCer), the first step in the biosynthetic pathway of GlcCer-based GSLs. This inhibitor is the *N*-alkylated imino sugar *N*-butyldeoxynojirimycin (NB-DNJ) (*5*, *6*) (Fig. 1). This compound is water soluble and noncytotoxic over a broad range of concentrations in vitro and in vivo. Its oral administration to healthy mice results in GSL depletion in multiple organs, without causing any overt pathology in the treated animals (*7*).

The recently described mouse model of Tay-Sachs disease (*8*) has allowed the evaluation of NB-DNJ as a potential therapeutic agent in vivo. Tay-Sachs disease results from mutations in the *HEXA* gene, which encodes the α subunit of β-hexosaminidase. These mutations result in a deficiency in the A isoenzyme, which is responsible for the degradation of G_{M2} ganglioside. When this enzyme is deficient in humans, G_{M2} ganglioside accumulates progressively and leads to severe neurological degeneration (*9*). In the mouse model of Tay-Sachs disease (generated by the targeted disruption of *Hexa*), the mice store G_{M2} ganglioside in a progressive fashion, but the concentrations never exceed the threshold required to elicit neurodegeneration (*8*). This is because in the mouse (but not human), a sialidase is sufficiently abundant that it can convert G_{M2} to G_{A2}, which can then be catabolized by the hexosaminidase B isoenzyme (*10*). This model therefore has all the hallmarks of Tay-Sachs disease, in that it stores G_{M2} ganglioside in the central nervous system (CNS), but it never develops the neurological symptoms characteristic of the human disease (*8*, *10*, *11*).

In this study, Tay-Sachs mice were reared on standard mouse chow up to the age of weaning (4 weeks postpartum), when they were placed on a powdered mouse chow diet containing NB-DNJ (*12*). No toxicity was observed in response to NB-DNJ administration on the basis of visible inspection and observation of the animals and of organ weights at autopsy. The only observed changes were in the lymphoid tissues (spleen and thymus) which were 50% acellular in the NB-DNJ–treated Tay-Sachs mice (*7*). In neither study was there any indication of immunocompromization as a result of this change in the cellular composition of these organs. The biochemical basis for these changes in lymphoid tissues is currently under investigation. A dosing regime of 4800 mg per kilogram of body weight per day in the Tay-Sachs mice gave serum concentrations in the region of 50 μM, as determined by mass spectrometry (*7*). Similar serum concentrations (steady-state trough concentration of ~20 μM) were achieved in humans during the evaluation of this compound as an antiviral agent when patients were treated with 43 mg per kilogram of body weight per day (*13*). The pharmacokinetics of NB-DNJ are two orders of magnitude poorer in mouse relative to human, necessitating high dosing regimes in the mouse in order to achieve serum concentrations in the predicted therapeutic range of 5 to 50 μM for the GSL storage disorders (*5*–*7*). The basis for this species-specific difference is currently unknown but may reflect higher rates of renal excretion of the drug in the mouse, relative to the human. We have found in previous studies in vivo that serum concentrations of 5 to 50 μM NB-DNJ result in a 40 to 70% reduction in GSL biosynthesis in the periphery. Because only a small percentage of the serum-level compound dose crosses the blood-brain barrier, this peripheral dose was anticipated to be sufficient to inhibit GSL biosynthesis in the CNS by ~5 to 10%, which would potentially permit the residual enzyme activity present in the CNS to catabolize G_{M2} more fully.

The effects that drug administration had on G_{M2} storage in the Tay-Sachs mouse were therefore determined at various ages by extracting total brain lipids, separating the base-resistant GSL fraction by thin-layer chromatography (TLC) (*14*) (Fig. 2), and identifying the G_{M2} species on the basis of comigration with an authentic G_{M2} standard. By 4 weeks of age, a storage band corresponding to G_{M2} was detected in the

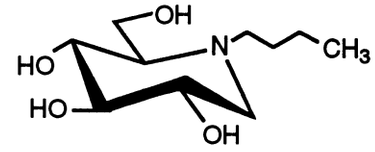

Fig. 1. Structure of *N*-(n-butyl)-1,5-dideoxy-1,5-imino-D-glucitol (*N*-butyl-deoxynojirimycin). Details of the enzyme inhibitory properties of this compound have been reviewed elswhere (*6*).

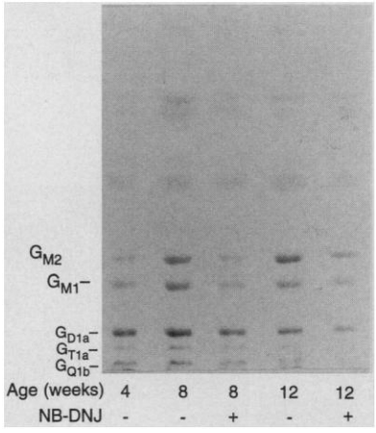

Fig. 2. TLC analysis of G_{M2} ganglioside storage in the Tay-Sachs mouse in the presence or absence of NB-DNJ. Mice were treated with NB-DNJ from 4 weeks of age up to 12 weeks, and their GSL profiles were compared at 4, 8, and 12 weeks relative to the untreated age-matched controls. Each lane on the TLC plate represents the base-resistant GSLs derived from the whole brain of an individual mouse, standardized to 5 mg dry brain weight per lane (*14*). The data are representative of studies carried out on five mice at each time point (*18*). The migration positions of authentic ganglioside standards are indicated.

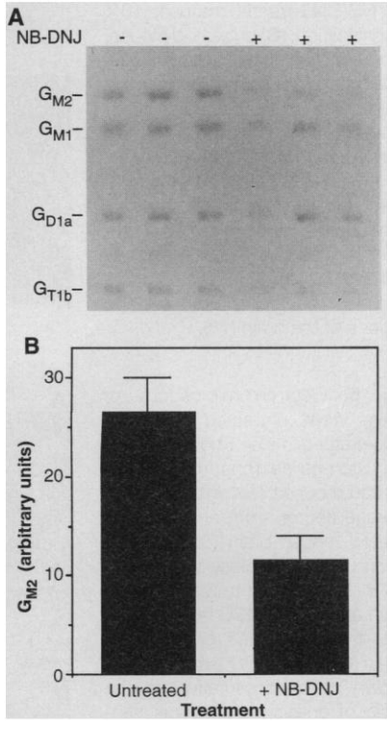

Fig. 3. Prevention of G_{M2} storage in 12-week-old mice. To demonstrate the variation in G_{M2} storage in mice treated with NB-DNJ a group of three untreated and three NB-DNJ–treated mice were compared at 12 weeks of age. (**A**) TLC profiles show total brain GSLs for three untreated mice (−) and three NB-DNJ–treated mice (+). (**B**) Scanning densitometry on the G_{M2} species from (A) is expressed in arbitrary units. The mean values ± standard deviation are shown.

untreated mice, in agreement with previous findings, and the accumulation of G_{M2} progressively increased with increasing age of the mice (*8*) (Fig. 2). However, in the 8-week-old mice that had been treated with NB-DNJ for 4 weeks after weaning, there was a reduction in the intensity of the G_{M2} ganglioside band, relative to the untreated age-matched controls, indicating that reduced amounts of storage were occurring in the presence of the drug. The mice were monitored for 12 weeks, and there was a consistent reduction in stored G_{M2} ganglioside in all animals from the NB-DNJ–treated group, irrespective of their age (Fig. 2). To examine the generality of these data, we evaluated a group of three untreated and three NB-DNJ–treated mice at 12 weeks (Fig. 3A). In all cases, the intensity of the G_{M2} band was significantly reduced in the NB-DNJ–treated animals, relative to the untreated age-matched controls. When scanning densitometry was performed on the TLC profiles, it was found that there was a ~50% reduction in G_{M2} ganglioside in the treated mouse brains relative to the untreated controls (Fig. 3B).

The neurons within the Tay-Sachs mouse brains that are responsible for the G_{M2} storage observed in whole brain lipid extracts are confined to certain specific regions of the brain (*11*). Therefore, we carried out cytochemical analysis on tissue sections from untreated mice and mice treated for 16 weeks with NB-DNJ, by means of periodic acid–Schiff (PAS) staining to detect the stored ganglioside within the storage neurons (*8*, *15*). It has previously been demonstrated in these mice that the distribution of neurons staining with PAS is coincident with neurons that immunostain with an antibody specific for G_{M2} ganglioside (*8*). In storage regions of the brain, such as the ventromedial hypothalamic nucleus, the NB-DNJ–treated mice had fewer PAS-positive neurons, and the intensity of staining in each neuron was reduced (Fig. 4, B and D), relative to the brain sections of untreated age-matched controls, which exhibited extensive storage (Fig. 4, A and C).

In storage neurons from untreated Tay-Sachs mouse brains (lateral septum and cortex) examined by electron microscopy (*16*), there were prominent regions of the cytoplasm containing large numbers of membranous cytoplasmic bodies (MCBs) containing the stored lipid product (Fig. 5A). In contrast, in the NB-DNJ–treated mice, it proved difficult to find storage neurons. However, when storage cells could be located, they contained MCBs with greatly reduced electron-dense contents (Fig. 5B). Because of extensive G_{M2} storage, sectioning of neurons from untreated mice frequently resulted in artifacts, with the storage product detaching partially from the surrounding membrane (Fig. 5A). In the NB-DNJ–treated mouse brains, the storage within neurons was always markedly reduced, relative to the untreated controls, and as a result, no sectioning artifact was observed (Fig. 5B). The NB-DNJ–treated mice had MCBs that contained less electron-dense storage lipid (Fig. 5D) but also did not have the prominent concentrically arranged lamellae characteristic of the MCBs in neurons from untreated mice (Fig. 5C). Instead, they exhibited a diffuse pattern of storage with membrane-like structures only clearly discernible in the periphery of the organelle (Fig. 5D). Taken together with the cytochemical data, this demonstrates that NB-DNJ prevents lysosomal storage and that the extent of storage per cell and per MCB is strongly reduced, in keeping with the biochemical data on whole brain GSLs (Figs. 2 and 3).

Our data here confirm our previous observation in normal mice (*7*) that oral treatment of mice with NB-DNJ is well tolerated and that it results in the predicted inhibition of GSL biosynthesis. Furthermore, we have been able to prevent storage of G_{M2} ganglioside in the Tay-Sachs mouse, as a consequence of reducing GSL biosynthesis. This indicates that NB-DNJ can cross the blood-brain barrier to an extent that can prevent storage. Because several of the human GSL storage diseases also involve the storage of GlcCer-based GSLs, theoretically, this therapeutic strategy could be applied to all of these disease states, irrespective of the specific storage product. This would include Gaucher (types 1, 2, and 3), Fabry disease, Tay-Sachs disease, Sandhoff dis-

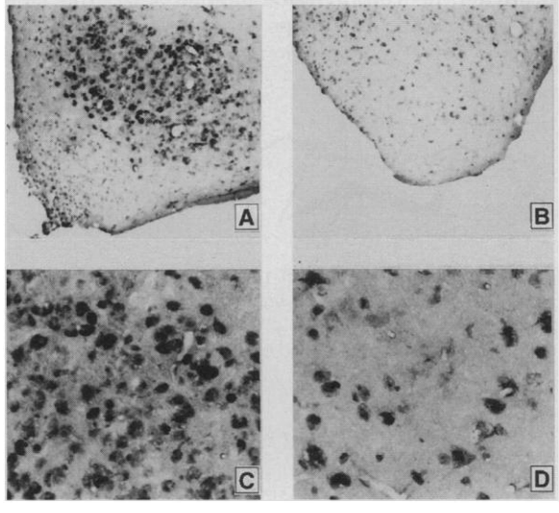

Fig. 4. G_{M2} storage in the ventromedial hypothalamus of untreated and NB-DNJ–treated mice (12 weeks of age). Frozen sections were stained with PAS to allow the visualization of G_{M2} storing neurons. Sections shown are (**A**) untreated mouse, 10× magnification; (**B**) NB-DNJ–treated mouse, 10× magnification; (**C**) untreated mouse, 25× magnification; and (**D**) NB-DNJ–treated mouse, 25× magnification. The sections were selected to ensure that sections from the two animals were at comparable coronal levels within the brain. The images shown are representative of data derived from four different pairs of mice. The reduction in PAS staining in NB-DNJ–treated mice was also observed in other storage regions of the brain (*18*).

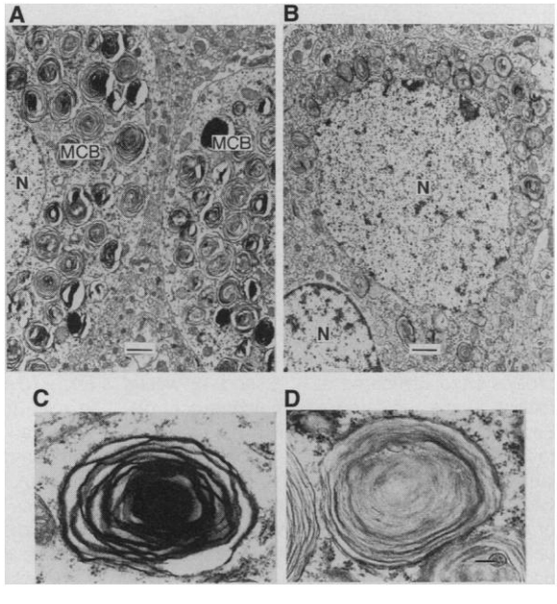

Fig. 5. Electron microscopy of brains from untreated and NB-DNJ–treated mice. Shown are (**A**) G_{M2} storage neurons from an untreated mouse brain and (**B**) a G_{M2} storage neuron from an NB-DNJ–treated mouse brain. Scale bar in (A) and (B), 1 μm. Close-up of (**C**) an MCB from an untreated mouse brain and (**D**) an MCB from an NB-DNJ–treated mouse brain. Scale bar in (C) and (D), 0.1 μm. The data shown are representative on the basis of analysis of multiple sections for multiple storage regions of the brain from two untreated and two NB-DNJ–treated animals, with the analysis carried out by two independent groups.

ease, G_{M1} gangliosidosis, and fucosidosis. Because this approach depends on the presence of residual enzyme activity, it would be anticipated to be most effective in juvenile, adult, and chronic forms of these diseases, rather than the infantile forms in which there is little or no residual enzyme activity. The current application of enzyme replacement to Gaucher disease is limited by the fact that the enzyme cannot cross the blood-brain barrier; hence, this therapy is only efficacious in type 1 disease where there is no neuropathology involved. NB-DNJ would not be anticipated to show efficacy in the treatment of Krabbe's disease and metachromatic leukodystrophy because both of these diseases involve the storage of galactosylceramide (GalCer)-based GSLs (GalCer and sulfatide, respectively). NB-DNJ fails to inhibit the galactosyltransferase that initiates the biosynthesis of this pathway (*17*). This is important when considering the use of this compound in humans because the formation of GalCer and sulfatide, which are both important constituents of myelin, will not be affected by NB-DNJ treatment, and therefore myelination and myelin stability should not be impaired. It will be of interest to determine which aspects of the various disease symptoms can be prevented or reversed with this approach. This will await testing of NB-DNJ in symptomatic mouse models of these diseases (*10*) and evaluation of NB-DNJ in the clinic.

REFERENCES AND NOTES

1. E. F. Neufeld, *Annu. Rev. Biochem.* **60**, 257 (1991).
2. E. Beutler, *Science* **256**, 794 (1992).
3. N. W. Barton *et al.*, *N. Engl. J. Med.* **324**, 1464 (1991).
4. E. Beutler *et al.*, *Blood* **78**, 1183 (1991).
5. F. M. Platt, G. R. Neises, R. A. Dwek, T. D. Butters, *J. Biol. Chem.* **269**, 8362 (1994); F. M. Platt, G. R. Neises, G. B. Karlsson, R. A. Dwek, T. D. Butters, *ibid.*, p. 27108.
6. F. M. Platt and T. D. Butters, *Trends Glycosci. Glycotechnol.* **7**, 495 (1995).
7. F. M. Platt, G. Reinkensmeier, R. A. Dwek, T. D. Butters, in preparation.
8. S. Yamanaka *et al.*, *Proc. Natl. Acad. Sci. U.S.A.* **91**, 9975 (1994).
9. K. Sandhoff, E. Conzelmann, E. F. Neufeld, M. M. Kaback, K. Suzuki, in *The Metabolic Basis of Inherited Disease*, C. R. Scriver, A. L. Beaudet, W. S. Sly, D. Valle, Eds. (McGraw-Hill, New York, 1989), vol. 2, pp. 1807–1839.
10. K. Sango *et al.*, *Nature Genet.* **11**, 170 (1995).
11. M. Taniike *et al.*, *Acta Neuropathol.* **89**, 296 (1995).
12. From weaning (4 weeks), mice were fed a diet of powdered mouse chow (expanded Rat and Mouse Chow 1, ground, SDS Ltd., Witham, Essex, UK) containing NB-DNJ. The diet and compound (both dry solids) were mixed thoroughly before use, stored at room temperature, and used within 7 days of mixing. Water was available to the mice ad libitum. The mice were housed under standard nonsterile conditions and were given 4800 mg per kilogram of body weight per day of NB-DNJ, which gave serum concentrations of ~50 μM (data not shown).
13. M. A. Fischl *et al.*, *J. Acquired Immune Defic. Syndr.* **7**, 139 (1994).
14. The animals were anesthetized, perfused with phosphate-buffered saline (PBS) (pH 7.2), and the intact brain removed. The brain tissue was manually homogenized in water, freeze-dried, and extracted twice with chloroform:methanol 2:1 (v/v) for 2 hours at room temperature and overnight at 4°C. A volume of the solvent extract equivalent to 5 mg dry weight for each brain was base hydrolyzed (*10*), and the Folch upper phase was separated by TLC (Silica gel 60 plates, Merck, British drug house, Poole, Dorset, UK) in chloroform:methanol: 0.22% calcium chloride (60:35:8), then sprayed with orcinol and visualized by heating to 80°C for 10 min.
15. Mice were anesthetized, perfused with PBS (pH 7.4) containing 4% paraformaldehyde, and the brain dissected and retained in fixative overnight prior to cryopreservation and sectioning. Frozen brain sections (7 μm) were warmed to room temperature, stained with PAS according to the manufacturer's instructions (Sigma, Poole, Dorset, UK), counterstained with Erhlich's hematoxylin, and mounted in diethyl-(phenyl)xanthine (British drug house).
16. The mice were anesthetized and perfusion fixed with 2% paraformaldehyde, 2% glutaraldehyde mix in PBS. The brain was dissected and fixed in the same fixative overnight at 4°C. The brain was trimmed, and 100-μm sections were cut on a vibrotome, then washed three times in 0.1 M phosphate buffer and stained with osmium tetroxide (1% in 0.1 M phosphate) for 35 min. The sections were dehydrated through an ethanol series, treated with propylene oxide (twice for 15 min), and then placed in Durcupan resin overnight at room temperature, transferred to glass slides, and kept at 60°C for 48 hours. Storage areas of the brain were selected microscopically, cut out of the thick section with a scalpel blade, and transferred to propylene oxide and embedded in Embed 800 (Electron Microscopy Sciences, Fort Washington, PA). Sections were stained with uranyl acetate/lead citrate and observed with a Hitachi 600 microscope at 75 kV.
17. T. Butters, unpublished observation.
18. F. Platt, unpublished observation.

19. We thank Searle/Monsanto for NB-DNJ, J. Vass and D. Smith for excellent technical assistance, and C. Beesley for photography. The Glycobiology Institute is supported by Searle/Monsanto. F.M.P. is a Lister Institute Research Fellow.

26 December 1996; accepted 28 February 1997

Crystal Structure of the Nucleotide Exchange Factor GrpE Bound to the ATPase Domain of the Molecular Chaperone DnaK

Celia J. Harrison, Manajit Hayer-Hartl, Maurizio Di Liberto, F.-Ulrich Hartl, John Kuriyan*

The crystal structure of the adenine nucleotide exchange factor GrpE in complex with the adenosine triphosphatase (ATPase) domain of *Escherichia coli* DnaK [heat shock protein 70 (Hsp70)] was determined at 2.8 angstrom resolution. A dimer of GrpE binds asymmetrically to a single molecule of DnaK. The structure of the nucleotide-free ATPase domain in complex with GrpE resembles closely that of the nucleotide-bound mammalian Hsp70 homolog, except for an outward rotation of one of the subdomains of the protein. This conformational change is not consistent with tight nucleotide binding. Two long α helices extend away from the GrpE dimer and suggest a role for GrpE in peptide release from DnaK.

Molecular chaperones play an essential role in protein folding by preventing the misfolding and aggregation of folding intermediates (*1–3*). Several classes of molecular chaperones have been conserved in evolution, including the members of the Hsp70, Hsp90, and Hsp60 (chaperonin) families. Whereas the chaperonins form large oligomeric ring structures, members of the Hsp70 and Hsp90 families function as monomers or dimers.

DnaK, the *Escherichia coli* homolog of Hsp70, and the various eukaryotic Hsp70s act by binding and releasing extended peptide segments enriched in hydrophobic side chains. DnaK and its homologs are composed of an NH_2-terminal 42-kD ATPase domain and a COOH-terminal 25-kD peptide binding domain, the structures of which are known (*4*, *5*). The binding and release of peptides from DnaK is controlled by conformational changes induced by adenosine triphosphate (ATP) binding and hydrolysis in a mechanism that is not understood. In this reaction DnaK does not act alone but cooperates with two other factors, the chaperone DnaJ and the nucleotide exchange factor GrpE (*6*), in a manner that is analogous to the regulation of many guanosine triphosphate binding proteins.

The following model of the DnaK reaction cycle in protein folding is now emerging (*7*): ATP-bound DnaK is characterized by rapid peptide binding and release (*8*). DnaJ stimulates the hydrolysis of ATP by

C. J. Harrison and J. Kuriyan, Laboratories of Molecular Biophysics and Howard Hughes Medical Institute, Rockefeller University, 1230 York Avenue, New York, NY 10021, USA.
M. Hayer-Hartl, M. Di Liberto, F.-U. Hartl, Cellular Biochemistry and Biophysics Program, Howard Hughes Medical Institute, and Memorial Sloan-Kettering Cancer Center, 1275 York Avenue New York, NY 10021, USA. After 15 June 1997, these authors will be at Max-Planck-Institute for Biochemistry, Am Klopferspitz 18A, 82152 Martinsried, Germany.
*To whom correspondence should be addressed.